

# Influence of Insertion Devices on the Beam Dynamics of DORIS III

Winfried Decking  
 DESY -MPY-  
 Notkestraße 85  
 D - 22603 Hamburg

## Abstract

The electron/positron storage ring DORIS III is operated routinely with up to 10 insertion devices to produce synchrotron radiation, mainly in the x-ray region. The influence of these wigglers on the electron beam dynamics was studied by measurements and tracking calculations.

In this paper an overview of the observed effects is given and compared with results obtained by 6-dimensional tracking calculations.

## 1 INTRODUCTION

DORIS III is a state of the art first generation synchrotron light source [1]. Originally dedicated to high energy physics, it has been operating since May 1993 solely as a synchrotron radiation source. To increase the number of beam lines by providing more space for insertion devices, the so-called 'Bypass' was constructed in one of the two straight sections of the racetrack shaped ring. This led to a total number of 10 built-in insertion devices, covering approximately 10% of the ring length. Table 1 gives an overview of the main storage ring parameters, especially stressing the optical functions in the 'Bypass'.

Table 1: Parameters of DORIS III

circumference	289 m
energy	4.5 GeV
beam current	$\approx 100$ mA in 5 Bunches
Emittances	
$\epsilon_x$	$0.44 \pi$ mrad mm
$\epsilon_z/\epsilon_x$	2% - 4%
$\Delta p/p$	0.1%
Optical Functions at ID-positions	
$\beta_x = 5 - 22$ m	$\beta_y = 5 - 21$ m
$D_x = 20 - 80$ cm	$D_y = 10 - 20$ cm

Note the horizontal and vertical dispersion, the latter is produced by the vertical bending, an artifact of the former HEP experimental area.

Wigglers do act in different ways on the beam dynamics. Starting with the ideal wiggler fields given by Halbach [2], one obtains equations of motion for a particle traveling through a wiggler [3], which describe

- linear focusing ( $\frac{1}{f} \sim (\frac{B_y}{p})^2$ ) leading to tune shifts and optic disturbances

- a nonlinear pseudo octupole term ( $\propto (\frac{B_y}{p})^2$ ) driving 4th order resonances of the kind  $4Q_{x,y}, 2Q_x \pm 2Q_y$ .

In table 2 these two terms together with some other properties of the DORIS insertion devices are summarized. It is obvious that the high field but long period wigglers have stronger linear effects, while the short period undulator should have stronger nonlinear effects.

As pointed out in [4], sextupoles can drive synchro-betatron resonances of 3rd order, if there is horizontal and vertical dispersion at the locations of the sextupoles. Similarly, the pseudo octupole term together with dispersion in the wigglers drives 4th order synchro-betatron resonances of the form

$$\begin{array}{ll}
 2Q_x \pm Q_y \pm Q_s, & \text{driven by } D_y \\
 Q_x \pm 2Q_y \pm Q_s, & D_x \\
 Q_x \pm Q_y \pm 2Q_s, & D_x D_y \\
 3Q_x \pm Q_s, & D_x \\
 3Q_y \pm Q_s, & D_y.
 \end{array}$$

These resonances turned out to be the most limiting effects while operating DORIS with insertion devices.

In addition to these 'intrinsic' effects, the fringe fields and field errors influence the beam dynamics.

## 2 EFFECTS ON BEAM DYNAMICS

### 2.1 Linear Effects

Due to the high energy of DORIS III, the disturbance of the linear optic is small. The vertical tune is shifted by  $\Delta Q_y \approx .07$  when all wigglers are closed. This is corrected by a global tune correction, leading to an average  $\beta_y$ -beat of  $\approx 10\%$ .

### 2.2 Intrinsic Nonlinear Effects

By closing the wigglers the operating area in the tune diagram decreases to values of  $\Delta Q_{x,y} = \pm 0.01$ . To understand the limitations in the surroundings of the working point, the limiting resonances were identified by measuring the dependence of the lifetime on the tunes. A list of the observed and identified resonances is given in table 3. At nearly every resonance the beam is completely lost. The most disturbing resonances are the 4th order synchro-betatron resonances, as predicted from the equations of motion. Some resonances (like the  $Q_x \pm 3Q_y$ ) cannot be explained by the ideal wiggler fields and must be driven by field errors or attributes of the wiggler fields which are not considered in the 'Halbach' formulas [2].

Table 2: List of Insertion Device Parameters

Name of ID	$\lambda$ cm	Number of Periods	$B_0$ T	Gap cm	$1/f$ m <sup>-1</sup>	$\sigma$ m <sup>-3</sup>	$K$	$E_c$ KeV	#
X-Ray Wiggler	14.0	28	1.17	3.0	.012	4.0	13.6	15.8	4
Hard X-Ray Wiggler	22.6	17	2.0	20	.036	4.6	34.0	27.0	1
Asymmetric Wiggler	22.0	18	1.17	3.0	.005	0.7	15.0	15.7	1
Triple XUV Undulator	9.-18.6	44-21	$\approx 0.6$	3.0	.003	2.5	4.7-11.5	7.5-8.9	1
X-Ray Undulator	3.14	127	0.8	1.4	.006	40	2.25	10.8	1
HARWI	24.	10	1.25	3.0	.008	0.9	26.9	16.1	1
Wiggler-Undulator	13.2	16	0.6	3.4	.002	0.8	7.4	8.1	1
Mini-Wiggler	12.	4	0.3	5.8			3.5	4.2	1
Bending Magnet			1.25					16.8	24

Table 3: Observed resonances  $lQ_x + mQ_y + nQ_s = \text{integer}$ . The resonance width is the difference between the two tunes where the lifetime reaches 1 hour on both sides of the resonance.

Order	Resonance $l, m, n$	Resonance width without	Resonance width with Wignlers
2	$1, \pm 1, 0$	$\approx .015$	$\approx .025$
3	$1, \pm 1, 1$	$\approx .010$	$\approx .020$
	$2, \pm 1, 0$	.004	.006
	$0, 3, 0$	.002	.002
4	$1, \pm 1, 2$	$0-.005$	.010-.020
	$1, 2, 1$	0	.002
	$2, \pm 1, \pm 1$	.002-.005	.005-.010
	$2, \pm 2, 0$	.005	.005-.010
	$1, \pm 3, 0$	0	.003
	$0, 4, 0$	0	.002 <sup>1</sup>
	$0, 3, \pm 1$	0	<sup>2</sup>

In addition to the listed resonances, decreases of lifetime which do not coincide with resonances up to 4th order are also observed. Most of them fit into crossing points of 5th order synchro-betatron resonances.

All these resonances are mainly driven by the X-Ray Wignlers and not by the X-Ray Undulator, which has the strongest nonlinearity but is located at a position with low  $\beta_y$  ( $\approx 5\text{m}$ ).

Similar resonance patterns are obtained with tracking calculations. The equations of motion [3] were inserted in the tracking code SIXTRACK [5], which allows fully 6-dimensional particle tracking.

Figure 1 shows the horizontal dynamic aperture evaluated from tracking runs with different wiggler settings.

The influence of the synchro-betatron resonances is clearly visible. If the tracking is done with vanishing dispersion at the wiggler locations, some of the synchro-betatron resonances vanish. Note also the decrease of the horizontal dynamic aperture from  $\approx 80\pi$  mrad mm to

<sup>1</sup>Only observed with bad vertical orbit.

<sup>2</sup>Only observed at points, where other resonances cross.

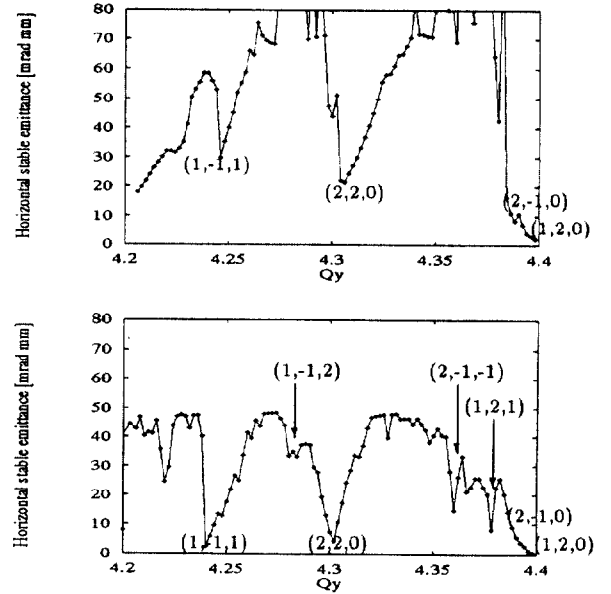


Figure 1: Horizontal dynamic aperture versus vertical tune obtained from tracking calculations. The other tune values are  $Q_x = 7.2$ ,  $Q_s = .041$ .

Upper: No wigglers.

Lower: 4 wigglers inserted at locations with high  $\beta_y$  and  $D_{x,y} \neq 0$ .

$\approx 40\pi$  mrad mm which is also observed in the machine. The vertical dynamic aperture remains constant, because it is determined by geometric restrictions.

### 2.3 Fringe Field Effects

Due to the finite width of the wiggler poles, the magnetic field depends on the horizontal position in the wiggler. This fact is illustrated in figure 2 where the field profile of one wiggler pole is plotted. At the bottom of the plot two  $6\sigma_x$  ellipses are sketched, one of them shifted by  $\approx 30\text{mm}$ . It is obvious, that for this case the particle paths will be in field regions which are not properly described by the 'Halbach' formulas [2], if the parameter used to describe

the field dependence on the horizontal coordinate is chosen to give good agreement in the central field region.

To investigate the effects of the fringe fields, one wiggler was operated off axis, e.g. was mounted  $\approx 15\text{mm}$  displaced from the beam axis. With the help of a symmetric orbit bump it was possible to change the electron orbit in the wiggler in a range of  $0 - 30\text{mm}$  with respect to the wiggler axis. A change of the resonance width of the sum resonance  $Q_x + Q_y$  was observed, as shown in figure 3.

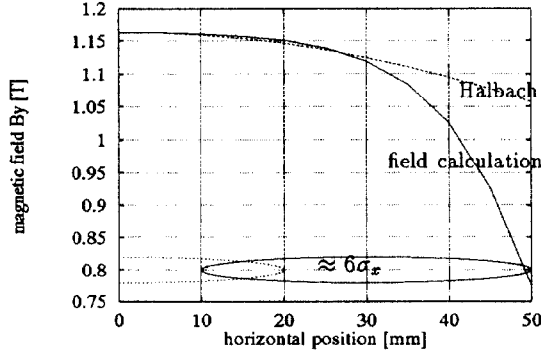


Figure 2: Field profile of the vertical field of one wiggler pole versus horizontal position.

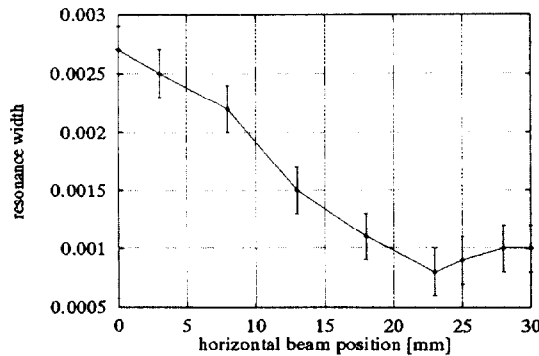


Figure 3: Resonance width of the sum resonance  $Q_x + Q_y$  versus horizontal closed orbit with respect to the wiggler axis.

The big  $\partial B_x / \partial x$  component of the fringe field leads to strong additional coupling. In this actual case, the additional coupling term compensates the coupling of the machine.

#### 2.4 Magnetic Field Errors

Unavoidable errors in the magnetic structure of a wiggler lead to magnetic field errors, which are normally represented by a multipole expansion of the measured field integrals  $\int B_{x,y} dz$ :

$$\int B_x dz - i \int B_y dz = \sum_n (a_n + ib_n)(x + iy)^n$$

Table 4: Upper limits of the field error multipoles

Multipole coefficient	Value	Criteria
$b_0$	200 Gcm	$\Delta \text{closed orbit} < 1/10\sigma_x$
$a_0$	50 Gcm	$\Delta \text{closed orbit} < 1/10\sigma_y$
$b_1$	400 G	$\Delta Q < \Delta Q_{\text{intrinsic}}$
$a_1$	30 G	additional coupling $< .1\%$
$b_2$	200G/cm	dynamic aperture
$b_3$	30G/cm <sup>2</sup>	$< \text{pseudo octupole}$
$b_4$	75G/cm <sup>3</sup>	dynamic aperture

with  $a_n$  = skew component and  $b_n$  = normal component.

From the beam dynamics point of view, it is sufficient to give upper limits for the multipole coefficients. These limits are evaluated by tracking and through other criteria. Table 4 gives a summary of the field error multipole limits evaluated for DORIS III.

Most of the measured multipole coefficients are below these limits. Due to this fact we expected only small influences of the field errors on the beam dynamics.

### 3 CONCLUSION

The main influence of the insertion devices at DORIS III are the excitations of additional synchro-betatron resonances, leading to a decrease of free tune space. Most of these resonances can be explained analytically as well as by tracking calculations using the ideal wiggler fields [2].

The fringe fields of a wiggler lead to additional coupling terms. This coupling was verified experimentally by measuring the change of the sum resonance width.

In addition, we observed some resonances (e.g.  $Q_x \pm 3Q_y$ ) which cannot be explained by the ideal field nor by integrated field errors.

### 4 ACKNOWLEDGMENTS

I want to acknowledge the contributions of O. Kaul, H. Nesemann and B. Sarau to the measurements and observations.

### 5 REFERENCES

- [1] H. Nesemann et al. First Experience with DORIS III. In *Proceedings of the XVth International Conference on High Energy Accelerators HEACC'92*, pages 549–551, 1992.
- [2] K. Halbach. Fields of undulators and wigglers. *Nuclear Instruments and Methods*, 187:109–177, 1981.
- [3] L. Smith. Effect of Insertion Devices on Beam Dynamics. *ESG TECH NOTE-24*, 1986.
- [4] A. Piwinski. Synchrotron Sidebands of Betatron Coupling Resonances. *DESY 93-189*, 1993.
- [5] F. Schmidt. SIXTRACK. *CERN/SL/91-52(AP)*, 1991.